



ELSEVIER

Journal of Chromatography A, 979 (2002) 105–113

JOURNAL OF
CHROMATOGRAPHY A

www.elsevier.com/locate/chroma

Micromachined capillary cross-connector for high-precision fraction collection

Julia Khandurina, András Guttman*

Torrey Mesa Research Institute, 3115 Merryfield Row, Suite 129, La Jolla, CA 92121-1125, USA

Abstract

A new approach for high-precision fraction collection of double-stranded DNA fragments by capillary electrophoresis coupled to a micromachined plastic capillary cross-connector is presented. The system design integrates four fused-silica capillaries with an acrylic cross-channel connector. The cross-channel structure was introduced to enhance the efficiency of the fraction collection process by electrokinetic manipulations. Following the detection of the sample zone of interest at or slightly upstream of the cross during the separation mode, the potentials were reconfigured to collection mode to direct the selected analyte zone into the corresponding collection vial, while keeping the rest of the sample components virtually stopped within the separation capillary. In this way the spacing between consecutive bands of interest can be physically increased, allowing precise isolation of spatially close sample zones. After collection of the target fraction the separation mode is resumed, and the separation/collection cycle is repeated until all desired sample zones are separated and captured. The capillary cross-connector was fabricated of a transparent acrylic substrate by microdrilling flat end and through channels, matching precisely the O.D. and I.D. of the connected capillary tubing, respectively. This design provided a close to zero dead volume connection assembly for the separation and collection capillaries causing minimal extra band broadening during high-precision micropreparative DNA fractionation.

© 2002 Elsevier Science B.V. All rights reserved.

Keywords: Instrumentation; Microfluidics; Chip technology; Fraction collection; DNA

1. Introduction

Capillary gel electrophoresis is an excellent separation tool, which also enables high-resolution micropreparative separation of biopolymers, such as DNA fragments [1–5]. The excellent resolving power of gel or polymer solution filled narrow bore channels readily provides sequencing grade separation of very similar size DNA molecules, usually detected by laser induced fluorescence [6]. Collec-

tion of any individual or all separated fragments by capillary electrophoresis (CE) proved to be feasible and provided enough material for such downstream processes as polymerase chain reaction (PCR), sequencing or cloning [4,7,8]. More recently, electrophoresis microchips were introduced as integrated microfluidic devices that enable precise fraction collection during electric field mediated separation of biologically important molecules, also benefiting in terms of miniaturization, reduced reagent consumption, speed and high-performance analysis [9,10]. In spite of the ease of electrokinetic manipulations in the microchannels enabling precise fraction sampling and collection, the length of the separation channel,

*Corresponding author. Tel.: +1-858-812-1052; fax: 1-858-812-1097.

E-mail address: andras.guttman@syngenta.com (A. Guttman).

and therefore the achievable resolving power, is limited. Another limitation imposed by the use of monolithic electrophoresis microchips is the lack of automation methods and robotic instrumentation readily adaptable to integrate these devices with the external macro-world and liquid connections necessary for high throughput processing and analysis.

The growing interest to connect variable length separation and transfer capillaries to microfluidic devices has necessitated the development of zero or low picoliter dead volume capillary connectors to maintain the high resolution subsequent to the junction. Connecting microfluidic devices to capillary columns is an important issue in mass spectrometry due to the need to efficiently process separated samples off the chip, while maintaining high separation performance for high resolution and sensitive MS analysis. Minimal or rather close to zero dead volume connections are required for transferring extremely small on-chip sample volumes. Recently, Zhang et al. introduced a microfabricated device to interface capillary electrophoresis (CE) with electrospray ionization mass spectrometry (ESI-MS). In this design, a modular and reuseable microdevice was coupled to an external subatmospheric electrospray interface using a liquid junction and a fused-silica transfer capillary [11]. A double etching procedure was used, and the fused-silica capillary was epoxy glued into the channel opening with the edge of the capillary being tapered to match the shape of the etched channel in order to minimize dead volume. In another approach, Lazar et al. have introduced a capillary below a T intersection perpendicular to the microchip plane [12]. Minimizing the dead volume associated with this capillary–chip junction was very critical to maintain the overall separation efficiency. Under optimized operating conditions, they observed only 25% increase in bandwidth. Figeys and Aebersold linked a transfer capillary perpendicular to a microfabricated device in such a way that the capillary also acted as an electroosmotic pump [13]. van der Moolen et al. reported a low dead volume micromachined injection device, connected to a fused-silica capillary allowing consecutive injections without current interruption [14]. The micromachined injection assembly was made of silicon and the channels were electrically isolated with a thin layer of silicon oxide to sustain electric fields up to 250

V/cm. Bings et al. [15] have significantly decreased the connection dead volume of a glass microfluidic device to a fused-silica capillary from the nanoliter to the picoliter scale by micromachining it with a flat-bottom shaped drill bit instead of a standard pointed one. Their approach apparently eliminated connection dead volume related band broadening.

For micropreparative CE applications, low dead volume coupling of the separation capillaries with specially designed microfluidic cross-connectors offers a powerful combination of microfluidic capabilities for analyte zone manipulation, including sampling and collection of fractions, with the advantages of using long separation channels. Here we report on an assembly, based on a plastic cross-connector device, coupled with four fused-silica capillaries for sample separation and fraction collection. Micromachining in plastic substrates enables fabrication of fine structures, including flat bottom end and through channels that are necessary to obtain minimal dead volume connection with narrow bore fused-silica capillaries. The assembly described in this work features integration of microfluidic functionality and long separation pathways, while minimizing necessary fluidic reservoirs and electrical connections for large-scale fraction collection.

2. Materials and methods

2.1. Cross-connector/capillary assembly

The cross-channel connector was fabricated of pre-shrunk acrylic MIL-P-5425 (National Jet, LaVale, MD, USA). The overall part size was $6 \times 6 \times 3$ mm ($0.236 \times 0.236 \times 0.118$ in.). A National Jet model 2M Ultrasensitive Microdrilling Machine and spade type microdrill bits were used. Four sets of holes converging to the center were drilled with Micrograin Tungsten Carbide drill bits: $360 \mu\text{m}$ (0.0142 in.) diameter counterbore, matching the O.D. of the fused-silica capillaries used, and $101 \mu\text{m}$ (0.0040 in.) diameter center hole matching the I.D. of the capillaries. The length of the wide and narrow channels corresponded to 2.5 and 1 mm, respectively (Fig. 1). Precise positioning while drilling and using special flat tip shape bits were essential to produce flat bottom holes, necessary to minimize the dead

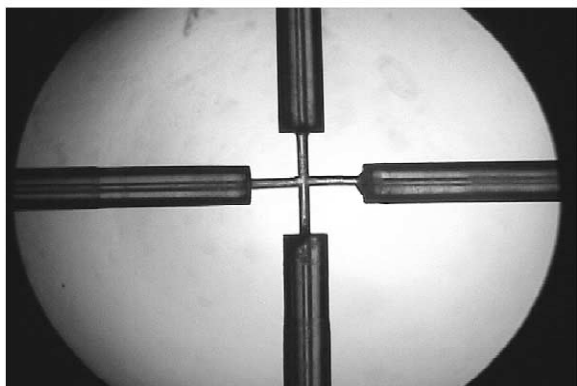


Fig. 1. Micromachined acrylic cross-connector coupled with four fused-silica capillaries.

volume of the capillary couplings. The ends of the fused-silica capillaries were sanded perpendicular and flat with a ceramic cutter (Beckman Instruments, Fullerton, CA, USA). In this work 360 μm O.D. \times 100 μm I.D. polyimide coated bare fused-silica capillary tubing (Polymicro Technologies, Phoenix, AZ, USA) was employed. Four pieces of 5 cm long capillaries were inserted into the micromachined acrylic cross-connector and fixed in place with epoxy, providing tight contact of the capillary ends with the narrow plastic channels.

2.2. Electrophoresis separation and detection setup

The acrylic cross-connector/capillary assembly was placed on the stage of an inverted epifluorescent microscope (Eclipse TE200, Nikon, Melville, NY, USA), and 0.2-ml microfuge tubes were used as buffer/sample reservoirs. Gold-plated beryllium electrodes provided electrical connections, and high voltage manipulations were accomplished with an in-house built four-channel, rapid ramp time power supply controlled by LabView software. The 532-nm beam of a frequency doubled NdYAG laser (GSF32-150, Intelite, Minden, NV, USA) was focused into the relevant position of the micromachined channel or capillary tubing with the microscope objective (10 \times , 0.45 NA), and the emitted fluorescent light was collected and collimated by the same objective and passed through a dichroic beam splitter, a bandpass filter and a spatial filter into a photomulti-

plier tube (PMT) detector (PRI, Products for Research, Danvers, MA, USA). The PMT output signal was amplified by a low noise current amplifier (model SR570, Stanford Research Systems, Sunnyvale, CA, USA), digitized by a PCI-6711 board (National Instruments, Austin, TX, USA), and acquired by a personal computer for subsequent processing with Caesar Workstation 7.0 software (CE Solutions, Mission Viejo, CA, USA). For imaging and monitoring fluidics movements at the larger areas of the cross-connector, 50 μM fluorescein dye solution (Sigma, St. Louis, MO, USA) was employed in conjunction with an argon-ion laser (Reliant 150m, Laser Physics, Salt Lake City, UT, USA). The laser output was filtered through a 488-nm laser filter (Edmund Scientific, Barrington, NJ, USA) and directed to the cross-connector at $\sim 45^\circ$ angle resulting in an ~ 2 mm diameter illumination spot. Fluidic movements were monitored visually, through the microscope eye piece, and the images were acquired using a digital video camcorder (Canon, Elura DV, Lake Success, NY, USA).

2.3. Chemicals

TBE buffer and ethidium bromide (EthBr) were obtained from Sigma (St. Louis, MO, USA). Appropriate amount of polyvinylpyrrolidone (PVP, M_r 1 300 000) (Aldrich, Milwaukee, WI, USA) was dissolved in 0.5 \times TBE buffer (45 mM Tris, 45 mM borate, 1 mM EDTA, pH 8.4), containing 0.5 μM EthBr, and used as a sieving medium for DNA separation and fractionation. The polymer solution was introduced into the cross-connector/capillary assembly with a syringe either by pressure or vacuum. The same polymer solution was used as running buffer in all reservoirs. All buffer and polymer solutions were filtered through 0.45- μm filters (Fisher, Pittsburgh, PA, USA).

Production of the various size DNA fragments by PCR is described elsewhere [16]. In brief, starting from 0.5 ng/ μl pUC19 template 101-, 187-, 299-, 427- and 567-base pairs (bp) fragments were amplified, using one common forward primer and five different reversed primers (0.5 μM each) in the reaction mixture of 1.5 mM MgCl_2 , 250 $\mu\text{g/ml}$ BSA, 20% glycerol, and 0.05 U/ μl Platinum Taq Polymerase (Life Technologies, Gaithersburg, MD,

USA). For re-amplification of collected fractions 5 μ l of the collected DNA fragment solutions in 0.5 \times TBE were added to the PCR cocktails.

2.4. Capillary electrophoresis

A single capillary instrument P/ACE MDQ Molecular Characterization System (Beckman Coulter, Fullerton, CA, USA) was used for CE analysis of the PCR fragments. Bare fused-silica capillaries, 100 μ m I.D., 30 cm total length (20 cm effective separation distance), filled with 2% PVP, 0.5 \times TBE, and 0.5 μ M EthBr sieving medium, were employed. DNA separations were conducted in reversed polarity mode (cathode at the injection side) at 25 $^{\circ}$ C under the following conditions: electrokinetic injection at 2 kV for 5 s; separation field strength 200 V/cm; laser-induced fluorescence (LIF) detection using an argon-ion laser (excitation wavelength: 488 nm, bandpass emission filter centered at 605 nm). PCR solutions were diluted in water 10-fold prior to injection. The data were acquired and processed by the 32 Karat software package (Beckman Coulter).

3. Results and discussions

In our earlier work we described fraction collection using a monolithic electrophoresis microchip device and demonstrated the feasibility of rapid and high-resolution micropreparative separation and collection of sample components by means of a simple cross-channel microchip [10]. Here we present an alternative configuration, where fused-silica capillaries are coupled to a plastic microfluidic cross-channel adaptor. Interfacing capillaries with microchips is advantageous since it combines high resolution CE separations with additional functionality and flexibility of the microfluidic manifolds while allowing the use of longer separation lengths. The idea is to enhance fractionation efficiency using microfluidics capabilities to create different electric fields within the interconnected manifold of capillary channels. Upon the detection of the analyte peak of interest at the cross, the potentials are reconfigured to collection mode to move the selected sample zone into the collection vial, while holding the rest of the sample components upstream in the separation path

halted or slowly migrating in the reverse direction. This method aims to increase spacing between the band being collected and the consecutive bands, providing enough time for collection manipulations and facilitating isolation of spatially close zones. Following the collection of the fraction of interest, the potentials are switched back to the separation mode until the detection of the next analyte peak. The separation/collection cycle can be repeated as necessary for collection of multiple fractions. Compared to multi collection-well chips, such cross-channel assembly should benefit from its simplicity, reduced number of fluidic reservoirs and electrodes, and readiness for automation, e.g. using interfacing capillaries with microtiter sample and fraction collection plates and robotics for large-scale and high throughput sample processing.

One of the main challenges in connecting narrow bore capillary columns with microfluidic structures is to minimize the dead volume in the joint. Such microfabrication process often involves complex multi-step photolithography/etching procedures or high-precision micromachining. The ability to assemble essentially zero dead volume connections is vital for adding extra functionalities to capillary electrophoresis based applications including sample pre-treatment, post-column reactions and analysis (e.g. MS), multi-dimensional separations and micropreparative fraction collection [17]. In this work we coupled fused-silica capillary tubing to a cross-connector, micromachined in plastic by drilling precisely centered small bore flat bottom and through channels in a cross configuration (Fig. 1). Acrylic plastic was chosen as substrate due to its excellent optical properties and chemical inertness. Taking into account the short channel length (\sim 1 mm) of the plastic portion of the system, filled with polymer solution medium, we did not expect significant distortions in the electrophoretic separation performance due to changes in the surface characteristics from fused-silica to plastic. The micromachining process is described in the Experimental section, and Fig. 1 shows the central area of the acrylic cross-connector with the inserted capillaries. As one can see, the flat bottom end shaped wider channels nicely accommodate the outer diameter (360 μ m) and ends of the capillaries. The cross-sectional area of the connector and the inner bores of the fused-silica

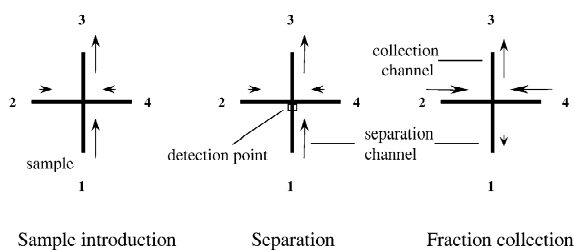


Fig. 2. Schematics of electrokinetic sample manipulations during sample introduction (left panel), separation (middle panel) and collection (right panel) modes using the cross-connector/capillary assembly. Arrows indicate direction and relative migration velocities of buffer/sample flow (not to scale).

capillaries (100 μm I.D.) are well matched, eliminating in this way band broadening effects related to any cross-sectional area changes.

Fig. 2 depicts the schematic representation of the sample introduction, separation and collection modes of the fraction collection process using the capillary cross-connector assembly. The sample was electrokinetically injected from port 1 into the separation capillary. Exemplary potential distribution during the different modes of the process, along with the electric fields created in the capillaries, are summarized in Table 1. During the separation step a small electric field was maintained in channels 2 and 4 to prevent analyte diffusion into the side channels. The detection window was placed slightly upstream ($\sim 100 \mu\text{m}$) of the actual channel cross. Upon detecting a peak of interest, the potentials were switched to

collection mode configuration (Table 1). During this step the selected sample zone was driven downstream to port 3 into the collection reservoir, while the rest of the sample components were halted in the separation channel upstream of the cross-connector. Maintaining zero or very small reversed electric field within the separation capillary prevented the consecutive sample zones from entering the collection channel, thus contaminating the fraction being collected. By this means, the spacing between the target fraction and the following fractions was increased enabling proper isolation of even closely migrating bands. Please note that, due to diffusion, additional band broadening of the halted analyte zones may occur when long collection times are applied.

Fig. 3 shows the fluidics manipulation within the acrylic cross-connector/capillary assembly in sepa-

Table 1
Electric potential distribution during the fraction collection cycle using acrylic cross-connector/capillary assembly

Ports/reservoirs	1	2	3	4
Capillary length, cm	5	5	5	5
Injection mode potentials, kV (E , kV/cm ^a)	0 (+0.045)	0.2 (+0.005)	0.5 (−0.055)	0.2 (+0.005)
Separation mode potentials, kV (E , kV/cm ^a)	0 (+0.180)	0.8 (+0.020)	2.0 (−0.220)	0.8 (+0.20)
Collection mode potentials, kV (E , kV/cm ^a)	0.7 (−0.005)	0 (+0.135)	2.0 (−0.265)	0 (+0.135)

^a Electric field strengths in the corresponding capillaries/channels. Positive and negative numbers refer to sample currents directed towards and from the cross, respectively.

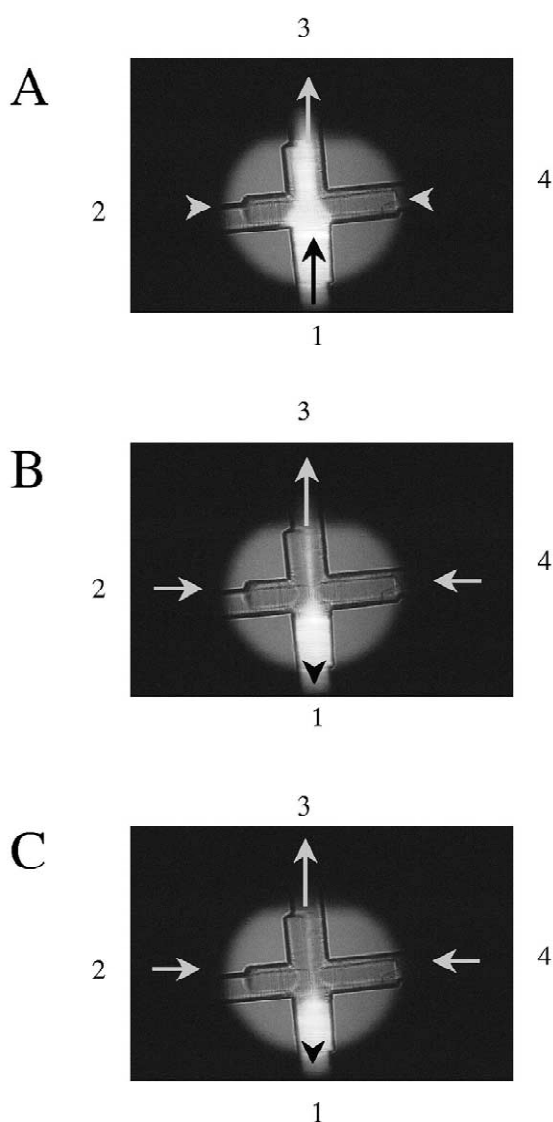


Fig. 3. Fluidics manipulation in the acrylic cross-connector/capillary assembly. (A) Separation mode, (B) collection mode immediately following the potential switch and (C) 10 s after the potential switch. The channels and reservoirs 2–4 were filled with $0.5\times$ TBE buffer containing 0.2% PVP. Reservoir 1 contained $50\ \mu\text{M}$ disodium fluorescein in $0.5\times$ TBE buffer. High voltage distribution is presented in Table 1.

ration (Fig. 3A) and collection modes (Fig. 3B,C). The images were taken using $50\ \mu\text{M}$ disodium fluorescein solution in TBE buffer in reservoir 1. The whole cross-connector/capillary assembly was filled

with $0.5\times$ TBE buffer containing 0.2% PVP to dynamically coat the capillary walls and suppress electroosmotic flow. The negatively charged dye molecules simulated the electrophoretic migration of DNA fragments. As one can observe, even and symmetrical flow of the fluorescein was obtained in the plastic portion of the system, undisturbed by the capillary joints and small imperfections of the cross-connector channels caused by a slight misalignment during the drilling process. After switching the potentials to collection mode (Table 1), a portion of the analyte zone was cut off and forwarded towards port 3 into the collection vial, while the rest of the sample components in the separation channel remained essentially still or very slowly migrating in the reverse direction. This latter is demonstrated by the image in Fig. 3C, which looks almost identical to Fig. 3B, but was actually acquired 10 s after the reconfiguration to the collection mode.

DNA fragments were separated by electrophoresis in capillary channel 1, using 2% PVP solution in $0.5\times$ TBE buffer as sieving medium ensuring both good separation performance and adequate dynamic coating of the capillaries. Ethidium bromide ($0.5\ \mu\text{M}$) was used as buffer additive to accommodate in migration labeling for LIF detection of the double-stranded (ds) DNA molecules. A $5\text{-}\mu\text{l}$ sample of 10-fold diluted PCR product mixture of 101-, 187-, 299-, 427- and 567-bp fragments, was placed into 0.2-ml microfuge tube and brought into contact with the separation capillary end and electrode 1, followed by the application of high voltage for 2–3 s for injection. Then, the sample tube was replaced by the running buffer reservoir, and the separation was performed by applying the high voltages as listed in Table 1. Fig. 4 shows the separation profiles obtained with the acrylic cross-connector/capillary assembly (upper trace) and the fused-silica capillary of the same separation length (lower trace) under otherwise identical electrophoresis conditions. The apparent similarity of the two traces reveals minimal extra band broadening caused by the cross-connector joint. The separation efficiencies of the cross-connector/capillary assembly and the uncoupled capillary column are compared in Table 2, demonstrating similar average theoretical plate numbers. Please note that irregularities and shoulders in the peak shapes introduced additional uncertainty and variability in the

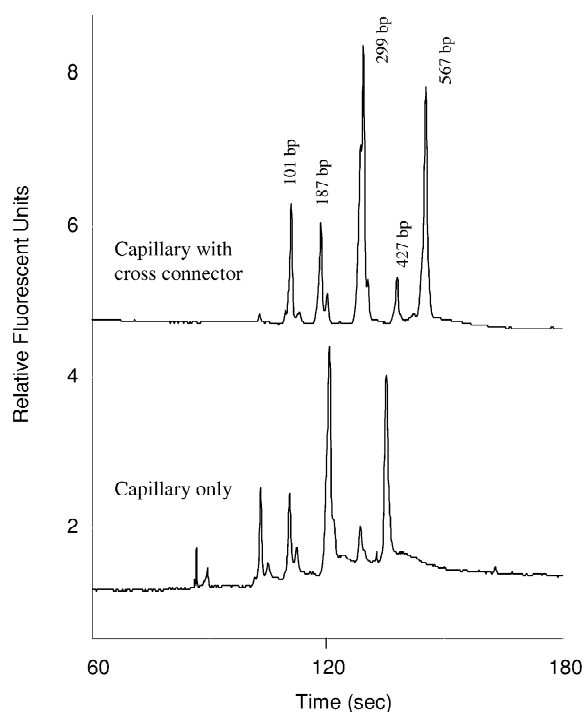


Fig. 4. Separation performance comparison using the cross-connector/capillary assembly and an equivalent length uncoupled capillary. In case of the coupled capillary, the detection point was set in the narrow channel of the cross-connector following the capillary/connector junction. Uncoated fused-silica capillaries: 100 μm I.D., 5 cm separation distance, 10 cm total length. Electric field strength in the separation channel: 180 V/cm. Separation medium: 2% PVP in 0.5 \times TBE containing 0.5 μM EthBr. Sample: 101-, 187-, 299-, 427- and 567-bp PCR product mix (10-fold dilution). Electrokinetic injection: 3 s at 0.5 kV.

Table 2
Separation efficiency of the uncoupled capillary and with cross-connector coupling

Peaks	N/m	
	Capillary	Cross-connector
101 bp	$2.62 \cdot 10^6$	$2.25 \cdot 10^6$
187 bp	$1.83 \cdot 10^6$	$1.72 \cdot 10^6$
299 bp	$0.85 \cdot 10^6$	$0.69 \cdot 10^6$
427 bp	$1.59 \cdot 10^6$	$1.53 \cdot 10^6$
567 bp	$1.24 \cdot 10^6$	$1.45 \cdot 10^6$

Average plate numbers per meter (N/m) over the course of five runs of the PCR product mix. Electrophoretic conditions were the same as in Fig. 4.

determination of the theoretical plate numbers. To investigate the effects of multiple separation/collection cycles on the separation performance, a four DNA fragment mixture was injected and separated, followed by the successive collection of the separated individual fragments. Fig. 5 superimposes the data acquisition profiles of an uninterrupted separation of the test mixture (trace A), and the interrupted separation and detection of the fastest DNA fragment (101 bp, trace B), followed by the potential reconfiguration to the collection mode (trace C, no peak) and resuming the separation step until the next DNA peak is registered (trace D). Then the separation/collection modes were alternated until all four fragments were successively isolated into separate collection vials (traces F and H). The corresponding collection mode traces are E, G and I (no peaks). The detection point was set at the same position in the entire course of the experiment, i.e. slightly upstream of the cross, as depicted in Fig. 2. PCR tubes containing 10 μl 0.5 \times TBE buffer were used as collection reservoirs, and collections were performed for 150 s to assure that the fractions reached the corresponding reservoirs. The durations of the collection steps were determined by the length of the collection capillary (5 cm) in the actual experimental set-up. Shorter collection capillaries and higher fields would definitely speed up the process and reduce diffusion related band broadening. The flat traces of C, E, G and I shown in Fig. 5 clearly demonstrate that no analyte leakage occurred during the fraction collection steps, and no analyte zones (other than the ones being collected), have passed the detection point. The long collection times employed in this experiment resulted in some analyte zone broadening, as can be observed in Fig. 5. Table 3 compares the theoretical plate numbers of the uninterrupted separation (trace A) and during the collection manipulations (traces B, D, F and H). Estimation of the additional band broadening (numbers not shown), resulted from the diffusion during the long collection times (assuming peak variance directly proportional to time), suggested that the actual experimental efficiency of the first two peaks (101 and 187 bp) can be worse than expected; however, for the larger fragments (299 and 567 bp) it can be higher. Considering this fact and the possible additional errors in theoretical plate number calculations due to

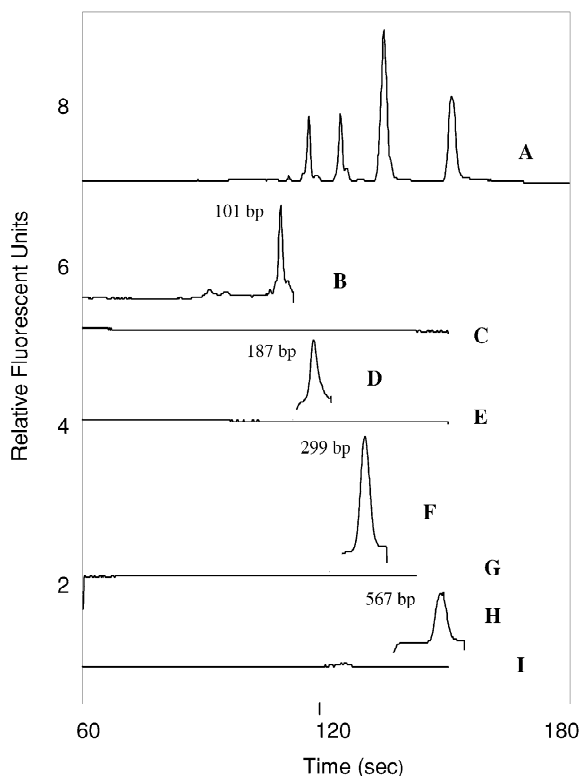


Fig. 5. Collection of multiple fractions by the cross-connector/capillary assembly. (A) Separation profile of the PCR product mixture. (B) Detection of the first (101-bp) peak followed by voltage reconfiguration to collection mode. (C) Detection trace during the collection step for the first fraction (101-bp). The flat line confirms that the larger DNA fractions were retained in the separation channel during the collection step. (D) Detection of the second peak (187 bp). (E) Trace during the collection of the second fraction. (F) Detection of the third peak (299 bp). (G) Trace during the collection of the third fraction. (H) Detection of the fourth peak (567 bp). (I) Trace during the collection of the fourth fraction. For better visualization of the process cycles, traces D, F and H were offset along *x*-axis by the values corresponding to the times of potential reconfiguration for the collection of the preceding peaks. Please note that the timing of the end point of separation trace B corresponds to the beginning of collection trace C; the same applies to traces D and E, and F and G, respectively. Separation distance 5 cm, with detection point slightly upstream of the cross. Conditions were the same as in Fig. 4. Potential distribution at the four ports during the cycles is summarized in Table 1. Sample: mixture of 101-, 187-, 299- and 567-bp PCR products (1:10 dilution of each in water).

peak shape irregularities suggests that observed band broadening and efficiency decrease during the fraction collection process may be caused by diffusional effects, within the experimental error. As emphasized

Table 3
Band broadening during collection of multiple fractions using the acrylic cross-connector/capillary assembly

Peaks	N separation	N collection
101 bp	92 000	65 900
187 bp	83 900	23 400
299 bp	34 500	17 700
567 bp	35 500	15 700

Separation and collection capillaries were 5 cm long. Potential distributions during the separation and collection modes are shown in Table 1. Collection time 2.5 min. Plate numbers of DNA fragment peaks during regular electrophoretic separation (N separation) and following collection cycles (N collection).

above, both shorter collection times and capillaries should alleviate the apparent decrease in peak efficiency.

Finally, in order to check for any cross contamination, each collected fraction was used as template for PCR re-amplification for the same fragment length using the corresponding set of primers (see Experimental section for details). The generated PCR products were then analyzed by a commercial capillary electrophoresis instrument (Fig. 6). The traces of the collected and re-amplified DNA fragments (E, F, G, H traces) correlate very well to the original fragments amplified directly from the pUC19 template (A, B, C, D traces), demonstrating the absence of cross contamination and the good efficiency of the proposed fraction collection method.

4. Conclusions

In this paper we introduced a new approach for high-precision fraction collection of DNA fragments using capillary electrophoresis in conjunction with an integrated acrylic cross-connector assembly. Fraction collection efficiency was improved by using the cross channel device for fluidic manipulations. Once an analyte zone has passed the detection window prior to the cross, the potentials were configured to collection mode, and the selected fraction was driven to the appropriate collection vial via a flexible sampling capillary. The voltage combination applied to the four fluidic ports ensured that the rest of the analyte components were retained in the separation channel upstream of the detection point, increasing

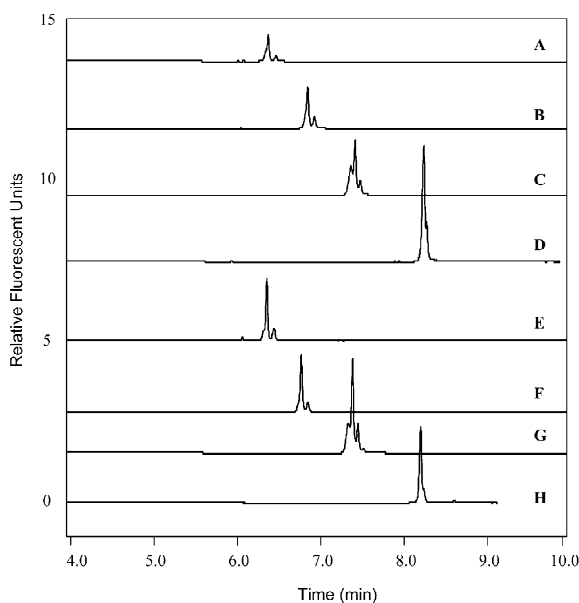


Fig. 6. Capillary electrophoresis analysis of the 101- (A), 187- (B), 299- (C) and 567- (D) bp PCR products using pUC19 template and PCR re-amplified DNA fractions collected using the cross-connector/capillary assembly (E: 101-, F: 187-, G: 299- and H: 567-bp fragments). LIF detection: excitation 488 nm, emission 605 nm. Capillary: 100 μm I.D., 20 cm separation distance, 30 cm total length. Separation matrix: 2% PVP, 0.5 \times TBE, 0.5 μM EthBr. Temperature: 25 $^{\circ}\text{C}$. Electrokinetic injection: 2 kV for 5 s. Separation field: 200 V/cm.

in this way the spacing between the fraction being collected and the immediately following band. Once the fraction of interest reached the corresponding collection vial, the potentials were switched back to the separation mode until the next sample zone was detected. The separation/collection cycle was repeated until all required fractions were physically isolated in the corresponding collection vials. The collected fractions were then subject to PCR amplification in order to check for possible cross contamination. All electrokinetic operations and potential switching were computer controlled. The cross-connector device was micromachined in plastic by drilling precisely centered flat bottom end channels which enable capillary coupling with essentially zero connection dead volume to maintain high separation efficiency. The suggested cross-connector design allows attachment of fused-silica capillaries of any

length, accommodating increased resolution needs. The flexible capillaries coupled to the cross-connector can be easily interfaced with sample and collection microtiter plates by robotically controlled positioning, further increasing automation and scale of analysis.

Acknowledgements

The authors greatly acknowledge the kind support of Syngenta Research and Technology.

References

- [1] A. Guttman, A.S. Cohen, D.N. Heiger, B.L. Karger, *Anal. Chem.* 62 (1990) 137.
- [2] A.W. Kuypers, P.M. Willems, M.J. van der Schans, P.C. Linszen, H.M. Wessels, C.H. de Bruijn, F.M. Everaerts, E.J. Mensink, *J. Chromatogr.* 621 (1993) 149.
- [3] S. Magnusdottir, C. Heller, P. Sergot, J.L. Viovy, *Electrophoresis* 18 (1997) 1990.
- [4] T. Irie, T. Oshida, H. Hasegawa, Y. Matsuoka, T. Li, Y. Oya, T. Tanaka, G. Tsujimoto, H. Kambara, *Electrophoresis* 21 (2000) 367.
- [5] P.O. Ekstrom, R. Wasserkort, M. Minarik, F. Foret, W.G. Thilly, *Biotechniques* 29 (2000) 582.
- [6] D.L. Smisek, *Electrophoresis* 16 (1995) 2094.
- [7] Z. Ronai, A. Guttman, *Am. Lab.* 32 (2000) 28.
- [8] M. Minarik, K. Kleparnik, M. Gilar, F. Foret, A.W. Miller, Z. Sosic, B.L. Karger, *Electrophoresis* 23 (2002) 35.
- [9] J.W. Hong, H. Hagiwara, T. Fuji, H. Machida, M. Inoue, M. Seki, I. Endo, in: J.M. Ramsey, A. van den Berg (Eds.), *Micro Total Analysis Systems 2001*, Kluwer, Dordrecht, 2001, p. 113.
- [10] J. Khandurina, T. Chovan, A. Guttman, *Anal. Chem.* 74 (2002) 1737.
- [11] B. Zhang, H. Liu, B.L. Karger, F. Foret, *Anal. Chem.* 71 (1999) 3258.
- [12] I.M. Lazar, R.S. Ramsey, S. Sundberg, J.M. Ramsey, *Anal. Chem.* 71 (1999) 3627.
- [13] D. Figeys, R. Aebersold, *Anal. Chem.* 70 (1998) 3721.
- [14] J.N. van der Moolen, H. Poppe, H.C. Smit, *Anal. Chem.* 69 (1997) 4220.
- [15] N.H. Bings, C. Wang, C.D. Skinner, C.L. Coyler, P. Thibault, D.J. Harrison, *Anal. Chem.* 71 (1999) 3292.
- [16] S. Schandrick, Z. Ronai, A. Guttman, *Electrophoresis* 22 (2001) 591.
- [17] J. Khandurina, A. Guttman, *J. Chromatogr. A* 943 (2002) 159.